



Optical properties of GaN/Er:GaN/GaN core–cladding planar waveguides

Yaqiong Yan, Zhenyu Sun, Weiping Zhao, Jing Li, Jingyu Lin, and Hongxing Jiang*

¹Department of Electrical and Computer Engineering, Texas Tech University, Lubbock, TX 79409, United States of America

*E-mail: hx.jiang@ttu.edu

Received May 16, 2019; revised May 30, 2019; accepted June 5, 2019; published online July 2, 2019

Erbium-doped GaN (Er:GaN) possesses superior optical, mechanical and thermal properties and is a very promising material as a gain medium for solid-state high-energy lasers. We report here the optical properties of GaN/Er:GaN/GaN core–cladding planar waveguides (PWGs). Optical confinement in the core layer has been investigated. The measured optical loss coefficients of Er:GaN PWGs at 1.54 μm are 1.0 cm^{-1} for the TE polarization mode and 1.2 cm^{-1} for the TM polarization mode. Approaches to further reduce optical loss and the optimal configuration for resonantly pumped GaN/Er:GaN PWGs for achieving amplification near 1.5 μm have been identified.

© 2019 The Japan Society of Applied Physics

The development of high-energy lasers (HELs) has been a subject of enormous research interest because of their broad applications in the fields of optical communications, industrial manufacturing and medicine. The optical gain medium plays a key role in a solid-state HEL.^{1,2)} The most common gain material for solid-state HELs today is synthetic garnet such as YAG doped with Nd (Nd:YAG) emitting at 1.06 μm . However, the lasing wavelength of 1.06 μm is not “retina-safe”, meaning that light at this wavelength is rather dangerous to vision, since it can be focused by the eye’s lens onto the retina, but the light is invisible and does not trigger the blink reflex.³⁾ Moreover, YAG as a host material has a relatively poor thermal conductivity of $\kappa \approx 14 \text{ W m}^{-1} \text{ K}^{-1}$ and a high thermal expansion coefficient of $\alpha \approx 7 \times 10^{-6} \text{ }^{\circ}\text{C}^{-1}$,⁴⁻⁶⁾ which hinders its ability to rapidly remove waste thermal energy from the laser host and thereby limits the power output and duty cycle performance of HELs. Er-doped YAG (Er:YAG) emitting at a 1.5 μm wavelength has attracted immense interest recently⁷⁻¹¹⁾ as a gain medium for HELs as this emission wavelength is strongly absorbed by the surface of the eye and is considered “retina-safe”. Furthermore, this wavelength has high transmission in air.¹²⁾ However, it is expected that Er:YAG possesses the same other disadvantages as Nd:YAG because the crystal host remains unchanged.

Er-doped GaN (Er:GaN) is a promising candidate as a gain medium for HELs operating at the “retina-safe” spectral region around 1.5 μm due to the outstanding thermal, mechanical and optical properties of the GaN host. Compared to YAG, GaN has a much higher thermal conductivity of $\kappa \approx 253 \text{ W m}^{-1} \text{ K}^{-1}$ and a smaller thermal expansion coefficient of $\alpha \approx 3.53 \times 10^{-6} \text{ }^{\circ}\text{C}^{-1}$.¹³⁾ Considering the thermal shock parameter, κ/α^2 , which is a rough measure of the maximum attainable lasing power for a solid-state laser attached to a heat sink,^{14,15)} a GaN host has the potential to provide a nearly two orders of magnitude enhancement in the maximum lasing power over YAG. Therefore, HELs based on an Er:GaN gain medium, if successfully realized, will represent a truly disruptive technology, which can overcome the limitations of the traditional Nd:YAG-based HELs.

To realize Er:GaN as a gain medium for HELs, Er:GaN in quasi-bulk crystal form is required to handle high power levels, meaning layer thicknesses in tens to hundreds of microns, to enable the fabrication of gain media in different geometries, such as disks, rods, and planar waveguides

(PWGs). However, progress has been made only recently in synthesizing Er:GaN quasi-bulk crystals with large thicknesses (up to $\sim 1 \text{ mm}$) by hydride vapor-phase epitaxy (HVPE).^{16,17)} These recent developments have made it possible for the first time to explore Er:GaN as a gain medium for HELs. The core–cladding PWG is one of the most desired geometries for the gain media of solid-state HELs.^{7,18-22)} The refractive index of Er-doped GaN increases almost linearly with an increase in the Er doping concentration (N_{Er}), following the relation of $n = n_0 + bN_{\text{Er}}$, where the value of $n_0 = 2.2735$ and $b = 0.00575 \times 10^{-20} \text{ cm}^3$.²³⁾ This property allows us to fabricate core–cladding PWGs by using an Er-doped layer as the core and undoped GaN as the cladding layers as illustrated in Fig. 1(a). For such a structure, the higher refractive index Er:GaN core material is sandwiched between the lower refractive index undoped GaN cladding materials, forming a PWG that confines optical radiation along the direction of propagation, and thereby allowing clad pumping to be employed. Moreover, a core–cladding PWG laser structure provides an efficient mechanism for waste heat removal because of its large lateral surface areas.

The performance of a GaN/Er:GaN/GaN PWG used as an optical amplifier can be described by the following expression:

$$G = \Gamma(g - \alpha)L, \quad (1)$$

where G , Γ , g , α , and L refer to the optical gain, the confinement factor, the gain coefficient of the active Er:GaN core layer, the optical loss coefficient, and the length of the PWG.²⁴⁾ Thus, in developing PWGs as gain media, the confinement factor and optical loss are the most important parameters. In this work, the optical confinement factor as a function of the Er:GaN core layer thickness and Er doping concentration was investigated and the results were used to guide the fabrication of GaN/Er:GaN/GaN core–cladding PWGs. The optical loss of the fabricated GaN/Er:GaN/GaN core–cladding PWGs was measured for both the TE and TM modes, using the measurement setup schematically shown in Fig. 1(b). From these results, we have identified an optimal configuration for clad pumping as well as approaches to further reduce optical loss.

Due to the fact that the size of Er atoms ($r_{\text{Er}} = 0.89 \text{ \AA}$) is larger than that of Ga atoms ($r_{\text{Ga}} = 0.62 \text{ \AA}$) and Er atoms are replacing Ga in Er:GaN, the Er:GaN layer grown on undoped GaN is expected to come under compressive strain and the

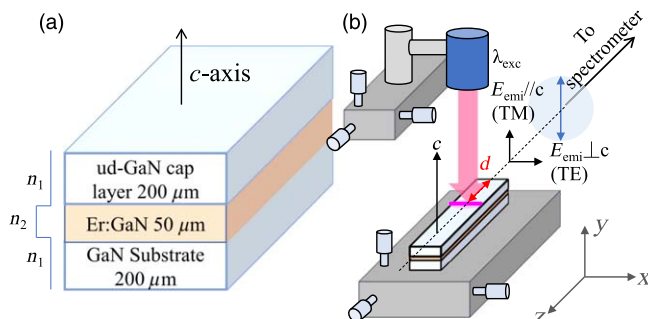


Fig. 1. (Color online) (a) Schematic diagram of GaN/Er:GaN/GaN PWG used in this work. The indices of refraction of the Er:GaN core and undoped GaN cladding layers around $1.5 \mu\text{m}$ are plotted to the left. (b) Schematic of experimental setup for optical loss measurements. The c -axis of GaN/Er:GaN/GaN is noted and E_{emi} stands for the polarization direction of emitted light.

material structure is expected to contain a certain amount of strain energy. It is expected that this strain energy will grow as the Er doping concentration and the thickness increase. As a result, it will eventually be more favorable for the Er:GaN layer to release strain through the generation of defects, which will increase the optical loss of GaN/Er:GaN/GaN PWGs. Therefore, a trade-off between structural parameters including the Er doping concentration and the thickness of the core layer for providing an adequate optical confinement factor but a small optical loss must be considered. To guide the HVPE growth, a detailed study was carried out by varying the thickness (d) and Er doping concentration (N_{Er}) in the core at a fixed cladding thickness of $200 \mu\text{m}$ and the results are summarized in Table I, which indicate that a GaN/Er:GaN/GaN PWG with a core thickness of $50 \mu\text{m}$ can attain a confinement factor of about 96% if the Er doping concentration in the core is about $3 \times 10^{19} \text{ cm}^{-3}$. To further illuminate the dependence of the confinement factor (Γ) on N_{Er} and d , we plot in Fig. 2 the confinement factor as a function of (a) N_{Er} for a core thickness of $d = 10, 30, 50, 70$ and $90 \mu\text{m}$ and (b) d for an Er doping concentration of N_{Er} varying from 10^{19} to 10^{21} cm^{-3} . The results indicate that a further increase in core thickness beyond $50 \mu\text{m}$ or in N_{Er} beyond $3 \times 10^{19} \text{ cm}^{-3}$ provides only a slight gain in performance but may significantly increase the amount of strain in the PWG layer structure. We expect that changes in the

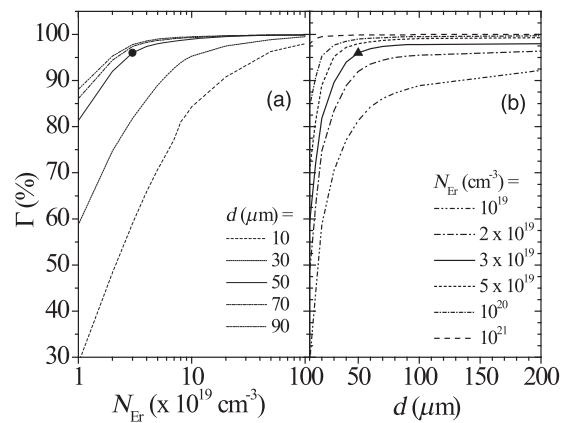


Fig. 2. Optical confinement factor (Γ) in the Er:GaN core at $1.54 \mu\text{m}$ as a function of (a) Er concentration (N_{Er}) for core thickness of $d = 10, 30, 50, 70$ and $90 \mu\text{m}$ and (b) core thickness d for Er doping concentration of N_{Er} varying from 10^{19} to 10^{21} cm^{-3} for a fixed thickness of cladding layers of $200 \mu\text{m}$. The PWG structure with $d = 50 \mu\text{m}$ and $N_{\text{Er}} = 3 \times 10^{19} \text{ cm}^{-3}$ employed in this study is highlighted with a solid dot and triangle.

confinement factor are negligibly small when the cladding layer thickness is increased beyond $200 \mu\text{m}$.

Based on the results shown in Table I and Fig. 2, we carried out HVPE growth for a core-cladding structure with a targeted $N_{\text{Er}} = 3 \times 10^{19} \text{ cm}^{-3}$ in the core.²⁵⁾ Figure 1(a) shows a schematic diagram of the GaN/Er:GaN/GaN PWG structure of this study. The undoped GaN cladding layer has a refractive index $n = 2.2735$ at $1.54 \mu\text{m}$, whereas the refractive index of the Er:GaN core layer is $n = 2.2752$ at $1.54 \mu\text{m}$ with an Er doping concentration of $3 \times 10^{19} \text{ atoms cm}^{-3}$.²³⁾ The refractive index profile of the PWG at $1.54 \mu\text{m}$ is also plotted to illustrate the physical basis of optical confinement in the core region along the c -axis of Er:GaN. The growth started with the deposition of a $20\text{-}\mu\text{m}$ -thick graded layer with an Er concentration linearly increasing from 0 to $3 \times 10^{19} \text{ atoms cm}^{-3}$ on an undoped GaN substrate about $300 \mu\text{m}$ in thickness, followed by the growth of a $100\text{-}\mu\text{m}$ -thick uniformly doped Er:GaN layer with an Er concentration of $3 \times 10^{19} \text{ atoms cm}^{-3}$. After HVPE growth, the top doped Er:GaN layer of the Er:GaN/GaN structure was subjected to mechanical and chemical-mechanical polishing (CMP) to bring it down to a thickness of $50 \mu\text{m}$.²⁵⁾ The quality of surface finishing is critical to providing low surface

Table I. Calculated optical confinement factor (%) in the Er:GaN core region of GaN/Er:GaN/GaN core-cladding PWGs with the core thickness (d) ranging from 5 to $200 \mu\text{m}$, and the Er doping concentration in the core (N_{Er}) ranging from 1×10^{19} to $1 \times 10^{21} \text{ atoms cm}^{-3}$. The undoped GaN cladding layer thickness is $200 \mu\text{m}$.

$d (\mu\text{m})$	$N_{\text{Er}} (\times 10^{19} \text{ cm}^{-3})$												
	1	2	3	4	5	6	7	8	9	10	20	50	100
5	10.3	23.7	33.4	40.6	46.4	50.8	54.8	57.9	59.7	60.6	76.2	88.0	93.1
10	28.7	48.3	59.0	65.9	70.7	74.2	77.2	81.0	82.7	84.3	90.8	96.3	98.0
15	43.8	62.8	72.0	77.5	81.1	84.0	85.9	87.9	89.3	90.6	95.9	98.2	99.1
20	58.8	74.7	81.8	85.9	89.0	91.1	92.7	93.9	94.7	95.3	97.5	98.9	99.5
30	70.5	83.5	89.6	93.2	95.2	96.1	96.7	97.1	97.4	97.7	98.8	99.5	99.7
40	77.1	88.9	94.0	96.3	97.2	97.6	98.0	98.2	98.4	98.5	99.3	99.7	99.8
50	81.3	92.0	96.0	97.4	98.0	98.3	98.5	98.7	98.9	99.0	99.5	99.8	99.9
60	84.3	93.6	96.9	98.0	98.4	98.7	98.9	99.0	99.1	99.2	99.6	99.8	99.9
70	86.1	94.4	97.4	98.3	98.7	98.9	99.1	99.2	99.3	99.3	99.7	99.9	99.9
80	87.3	95.0	97.6	98.5	98.9	99.1	99.2	99.3	99.4	99.4	99.7	99.9	99.9
90	88.1	95.3	97.8	98.6	99.0	99.2	99.3	99.4	99.4	99.5	99.7	99.9	99.9
100	88.9	95.5	97.8	98.7	99.1	99.2	99.3	99.4	99.5	99.5	99.8	99.9	100.0
200	92.2	96.4	98.0	98.8	99.3	99.5	99.6	99.7	99.7	99.7	99.9	100.0	100.0

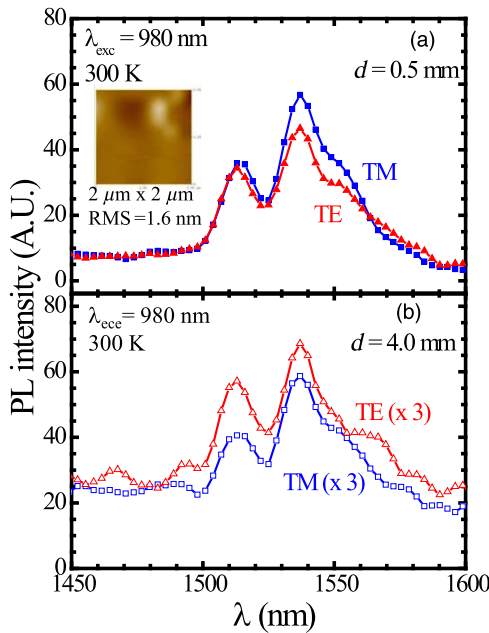


Fig. 3. (Color online) Photoluminescence (PL) emission spectra near $1.5 \mu\text{m}$ under a resonant excitation, $\lambda_{exc} = 980 \text{ nm}$, measured at the exit facet of the PWG with the laser excitation focused onto two different positions at distances, d , from the PWG's exit facet of (a) $d = 0.5 \text{ mm}$ and (b) $d = 4.0 \text{ mm}$. The inset of (a) is an AFM image of the top surface of the Er:GaN core layer after a CMP process and before regrowth of the top undoped GaN cladding layer.

scattering and hence low optical loss. The atomic force microscopy (AFM) image over a scanning area of $2 \mu\text{m} \times 2 \mu\text{m}$ shown in the inset of Fig. 3(a) reveals the morphology of the polished Er:GaN top surface, which indicates that we achieved a smooth surface for the Er:GaN core layer with an RMS roughness of 1.6 nm . After the CMP process, another $20 \mu\text{m}$ graded layer with an Er concentration linearly decreasing from $3 \times 10^{19} \text{ atoms cm}^{-3}$ to 0 and an undoped GaN cladding layer with a thickness of $300 \mu\text{m}$ were grown by HVPE on top of the Er:GaN core layer. After completion of the growth, all six sides of the GaN/Er:GaN/GaN core-cladding PWG were polished to mirror finishing using CMP processing. The PWG sample of this study has dimensions of 7 mm in length and 0.8 mm in width.

X-ray diffraction (XRD) characterization results reveal that the Er:GaN core layer has an FWHM of the ω -scan (rocking curve) for the GaN (002) diffraction peak of about 500 arcsec , which indicates that the Er:GaN core layer has a reasonably good crystalline quality. The XRD θ - 2θ scan of the GaN (0002) peak of Er:GaN appears at a smaller angle than that of the GaN substrate,¹⁶⁾ indicating that the core layer is under a compressive strain, as expected. The PWG was placed on an x - y - z stage as illustrated in Fig. 1(b). A 980 nm laser diode (LD) was used as an excitation source for generating PL emission in the PWG at $1.54 \mu\text{m}$. The $1.54 \mu\text{m}$ emission was then collected from the exit end of the PWG using an optical fiber ($400 \mu\text{m}$ in diameter) connected to a thermoelectric-cooled InGaAs infrared spectrometer. The separation distance between the laser excitation spot and the exit end of the PWG, d , can be varied continuously. A polarizer was placed in front of the optical fiber to measure the PL emission from the PWG in two different polarization configurations of the TM and TE modes in which the emitted

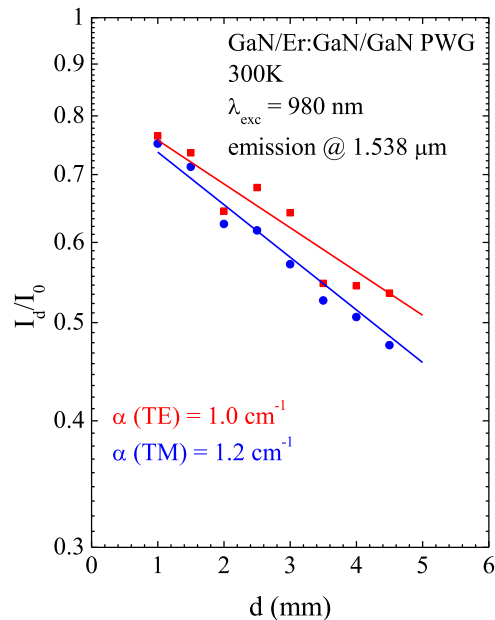


Fig. 4. (Color online) Normalized room-temperature PL emission intensities at $1.538 \mu\text{m}$ of TM and TE modes of Er:GaN/GaN/Er:GaN PWG under a resonant excitation, $\lambda_{exc} = 980 \text{ nm}$, as functions of d , the distance between the laser excitation spot and the PWG's exit facet. The solid circles and solid squares are the experimental data for the TM and TE modes respectively, and the solid lines are the least-squares fits of the data with Eq. (2).

photons were, respectively, in a configuration with the electrical field E parallel to and perpendicular to the c -axis. In GaN/Er:GaN/PWGs, the c -axis is always along the growth direction and perpendicular to the PWG's plane.

Figure 3 shows the PL spectra obtained for laser excitation focused onto two different positions at $d = 0.5 \text{ mm}$ (a) and $d = 4.0 \text{ mm}$ (b). Under 980 nm excitation, carriers are resonantly excited from the ground-state manifold ($^4\text{I}_{15/2}$) to the upper $^4\text{I}_{11/2}$ manifold of Er^{3+} ions. Three main emission lines at 1.514 , 1.538 , and $1.556 \mu\text{m}$ are clearly resolved, which result from the transitions between the Stark sublevels of the first excited state ($^4\text{I}_{13/2}$) and ground state ($^4\text{I}_{15/2}$)²⁶⁾ with the $1.538 \mu\text{m}$ emission line possessing the highest intensity. Interestingly, Fig. 3 shows that the TM mode has higher emission intensities for all the three emission lines measured at $d = 0.5 \text{ mm}$, which suggests that the TM mode has a higher excitation/absorption efficiency than the TE mode. For both the TM and TE modes, the PL emission intensities measured at $d = 4.0 \text{ mm}$ decrease compared to those at $d = 0.5 \text{ mm}$ since photons generated at the excitation spot need to travel a longer distance before getting detected. What is interesting is that the amount of reduction in emission intensity for the TM mode is greater than that for the TE mode, with the TM mode decreasing almost by a factor of 3 and the TE mode decreasing by a factor of about 2. Consequently, the TE mode exhibits higher emission intensities for all the three emission lines compared to the TM mode for PL signals measured at $d = 4.0 \text{ mm}$. The results shown in Fig. 3 can be understood by taking the optical loss of the PWG into consideration. Since the initial $1.538 \mu\text{m}$ emission intensities generated by the 980 nm LD at varying spots are the same for a given polarization mode, as the excitation spot moves farther away, the emitted photons at $1.538 \mu\text{m}$ must travel a longer distance before reaching the exit end of the waveguide. Thus, the emission intensity detected at the exit end of

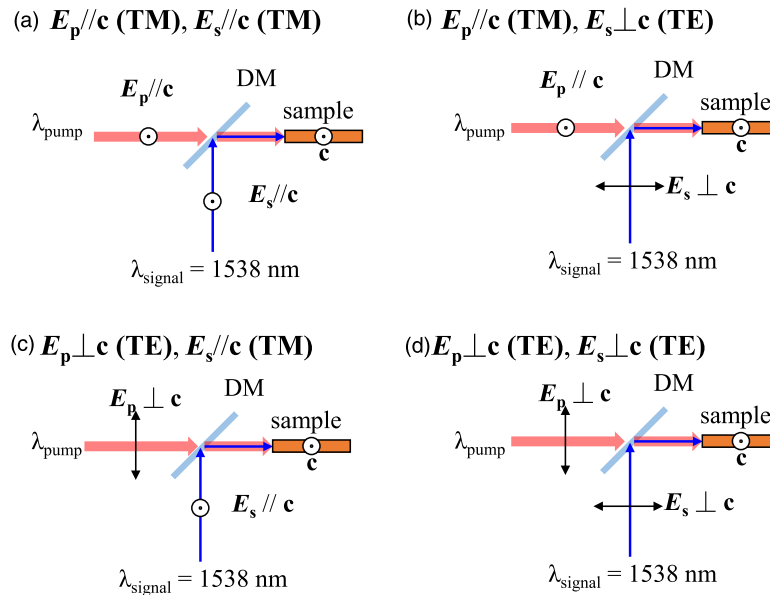


Fig. 5. (Color online) Four possible configurations for optical pumping of GaN/Er:GaN/GaN core-cladding PWGs, where E_p denotes the polarization of the pumping laser ($\lambda_{\text{pump}} = 980 \text{ nm}$) and E_s denotes the polarization of the signal laser ($\lambda_{\text{signal}} = 1538 \text{ nm}$): (a) $E_p/\!/c$ (TM) and $E_s/\!/c$ (TM); (b) $E_p/\!/c$ (TM) and $E_s\perp c$ (TE); (c) $E_p\perp c$ (TE) and $E_s/\!/c$ (TM); and (d) $E_p\perp c$ (TE) and $E_s\perp c$ (TE).

the PWG, I_d , is the signal that survives after propagation of a distance (d) and can be written as

$$I_d = I_0 e^{-\alpha d}, \quad (2)$$

where α denotes the optical loss coefficient. Figure 4 plots the dependence on d of the normalized $1.538 \mu\text{m}$ emission intensities measured in the TE and TM modes and the solid lines are the least-squares fits of data with equation (2). The results show that our GaN/Er:GaN/GaN PWGs have an optical loss of 1.0 cm^{-1} for the TE mode, and accordingly, a slightly higher optical loss of 1.2 cm^{-1} for the TM mode. Our results shown in Figs. 3 and 4 imply that emission intensity can be generated more efficiently in TM mode than in TE mode, but TM mode has a higher optical loss than TE mode. Higher optical loss is generally expected for the TM mode in most gain media and lasers.²⁷⁾ As the presence of defects related to strain is one of the dominant optical loss mechanisms, optimization of the graded layers between Er:GaN and undoped GaN cladding layers is expected to further improve the overall material quality and reduce the optical loss of GaN/Er:GaN/GaN core-cladding PWGs.

Our results provide valuable insights into the desired configurations to effectively excite GaN/Er:GaN/GaN PWGs to achieve gain and lasing. Possible configurations for the cladding pumping of GaN/Er:GaN/GaN core-cladding PWGs are shown in Fig. 5. By denoting E_p as the polarization of the pumping laser ($\lambda_{\text{pump}} = 980 \text{ nm}$) and E_s as the polarization of the signal laser ($\lambda_{\text{signal}} = 1538 \text{ nm}$), there are a total of four possible configurations for the optical pump, as shown in Fig. 5: (a) $E_p/\!/c$ (TM), $E_s/\!/c$ (TM); (b) $E_p/\!/c$ (TM), $E_s\perp c$ (TE); (c) $E_p\perp c$ (TE), $E_s/\!/c$ (TM); and (d) $E_p\perp c$ (TE), $E_s\perp c$ (TE). In consideration of the experimental results shown in Figs. 3 and 4, the optimum configuration for achieving optically pumped amplifiers/lasers based on GaN/Er:GaN/GaN core-cladding PWGs should be the configuration identified in Fig. 5(b) with $E_p/\!/c$ (TM) and $E_s\perp c$ (TE), which provides the maximum optical excitation efficiency and minimum optical loss.

In summary, the optical properties of GaN/Er:GaN/GaN core-cladding PWGs synthesized by HVPE have been studied near $1.5 \mu\text{m}$. For a PWG structure with a thickness of about $50 \mu\text{m}$ and an Er concentration of $3 \times 10^{19} \text{ atoms cm}^{-3}$ in the Er:GaN core, the optical loss coefficients at $1.538 \mu\text{m}$ were 1.0 cm^{-1} for the TE mode and 1.2 cm^{-1} for the TM mode. With the observation of a higher excitation efficiency for the TM mode and a lower optical loss for the TE mode, we have identified an optimal cladding pumping configuration for achieving optical amplification/lasing in GaN/Er:GaN/GaN core-cladding PWGs, which should consist of a pump laser polarization of $E_p/\!/c$ (TM) and a signal laser polarization of $E_s\perp c$ (TE). Optimization of the graded layers between Er:GaN and undoped GaN cladding layers is still needed to further reduce the optical loss of GaN/Er:GaN/GaN core-cladding PWGs.

The work is supported by the Directed Energy—Joint Transition Office Multidisciplinary Research Initiative program (grant #N00014-17-1-2531). H. X. Jiang and J. Y. Lin would also like to acknowledge the support of Whitacre Endowed Chairs by the AT&T Foundation.

- 1) Y. Kalisky and O. Kalisky, *Opt. Eng.* **49**, 091003 (2010).
- 2) J. A. Zuchlich, D. J. Lund, and B. E. Stuck, *Health Phys.* **92**, 15 (2007).
- 3) V. E. Kinsey, *Archives Ophthalmol.* **39**, 508 (1948).
- 4) R. Wynne, J. L. Daney, and T. Y. Fan, *Appl. Opt.* **38**, 3282 (1999).
- 5) H. Furuse, R. Yasuhara, and K. Hiraga, *Opt. Mater. Express* **4**, 1794 (2014).
- 6) W. Xie, S. C. Tam, H. Yang, J. Gu, G. Zhao, Y. L. Lam, and W. Tan, *Opt. Laser Technol.* **31**, 521 (1999).
- 7) N. Ter-Gabrielyan, V. Fromzel, X. Mu, H. Meissner, and M. Dubinskii, *Opt. Lett.* **38**, 2431 (2013).
- 8) J. O. White, *IEEE J. Quantum Electron.* **45**, 1213 (2009).
- 9) M. Nemec, J. Sulc, L. Indra, M. Fibrich, and H. Jelinkova, *Laser Phys.* **25**, 015803 (2015).
- 10) T. Sanamyan, *J. Opt. Soc. Am. B* **33**, D1 (2016).
- 11) D. J. Ottaway, L. Harris, and P. J. Veitch, *Opt. Express* **24**, 15341 (2016).
- 12) J. Bailey, A. Simpson, and D. Crisp, *Publ. Astron. Soc. Pac.* **119**, 228 (2007).
- 13) H. Shibata, Y. Waseda, H. Ohta, K. Kiyomi, K. Shimoyama, K. Fujito, H. Nagaoka, Y. Kagamitani, R. Simura, and T. Fukuda, *Mater. Trans.* **48**, 2782 (2007).
- 14) D. C. Brown, *IEEE J. Quantum Electron.* **33**, 861 (1997).
- 15) T. Taira, *C. R. Phys.* **8**, 138 (2007).

- [16] Z. Y. Sun, J. Li, W. P. Zhao, J. Y. Lin, and H. X. Jiang, *Appl. Phys. Lett.* **109**, 052101 (2016).
- [17] Z. Y. Sun, L. C. Tung, W. P. Zhao, J. Li, J. Y. Lin, and H. X. Jiang, *Appl. Phys. Lett.* **111**, 072109 (2017).
- [18] M. Digonnet, C. Gaeta, D. O'meara, and H. Shaw, *J. Lightwave Technol.* **5**, 642 (1987).
- [19] V. Sudesh, T. McComb, Y. Chen, M. Bass, M. Richardson, J. Ballato, and A. E. Siegman, *Appl. Phys. B* **90**, 369 (2008).
- [20] A. E. Siegman, *J. Opt. Soc. Am. B* **24**, 1677 (2007).
- [21] J. I. Mackenzie, C. Li, D. P. Shepherd, H. E. Meissner, and S. C. Mitchell, *Opt. Lett.* **26**, 698 (2001).
- [22] A. Okhrimchuk, V. Mezentsev, A. Shestakov, and I. Bennion, *Opt. Express* **20**, 3833 (2012).
- [23] S. Alajlouni, Z. Y. Sun, J. Li, J. M. Zavada, J. Y. Lin, and H. X. Jiang, *Appl. Phys. Lett.* **105**, 081104 (2014).
- [24] K. Gerd, *Optical Fiber Communications* (McGraw-Hill, New York, 1998).
- [25] Z. Y. Sun, Y. Q. Yan, T. B. Smith, W. P. Zhao, J. Li, J. Y. Lin, and H. X. Jiang, *Appl. Phys. Lett.* **114**, 222105 (2019).
- [26] M. Stachowicz, A. Kozanecki, C. G. Ma, M. G. Brik, J. Y. Lin, H. X. Jiang, and J. M. Zavada, *Opt. Mater.* **37**, 165 (2014).
- [27] H. Tanaka, A. Watabe, J. Shimada, Y. Katagiri, and Y. Suzuki, U.S. Patent 5,497,390 (1996).